Supplemental Material of Structural Identification of Piecewise-Linear Models of Genetic Regulatory Networks

Riccardo Porreca [1], Samuel Drulhe [2], Hidde De Jong [2], Giancarlo Ferrari-Trecate [1]

[1]Dipartimento di Informatica e Sistemistica, Università degli Studi di Pavia,
via Ferrata 1, 27100 Pavia, Italy
{riccardo.porreca, giancarlo.ferrari}@unipv.it

[2] INRIA Grenoble-Rhône-Alpes, 655 avenue de l'Europe, Montbonnot,
38334 Saint-Ismier Cedex, France
{Samuel.Drulhe, Hidde.de-Jong}@inrialpes.fr

1 Model equations and parameter values

The PL model of the carbon starvation response network in Fig. 5 in the main text consists of the following equations [2], where the variables x_{Cya}, x_{CRP}, x_{Fis}, x_{GyrAB}, x_{TopA}, and x_{rrn} denote the concentrations of Cya, CRP, Fis, GyrAB, TopA, and stable RNAs, respectively, while u_{s} represents the carbon starvation signal. In particular, $s^+(u_{\mathrm{s}}, \theta_{\mathrm{s}}) = 1\,(0)$ denotes the presence (absence) of the carbon starvation signal.

$$
\begin{aligned}
\dot{x}_{\mathrm{Cya}} &= \kappa^1_{\mathrm{Cya}} + \kappa^2_{\mathrm{Cya}}\,(1 - s^+(x_{\mathrm{CRP}}, \theta^2_{\mathrm{CRP}})\,s^+(x_{\mathrm{Cya}}, \theta^2_{\mathrm{Cya}})\,s^+(u_{\mathrm{s}}, \theta_{\mathrm{s}})) - \gamma_{\mathrm{Cya}}\,x_{\mathrm{Cya}} \\
\dot{x}_{\mathrm{CRP}} &= \kappa^1_{\mathrm{CRP}} + \kappa^2_{\mathrm{CRP}}\,s^-(x_{\mathrm{Fis}}, \theta^2_{\mathrm{Fis}})\,s^+(x_{\mathrm{CRP}}, \theta^1_{\mathrm{CRP}})\,s^+(x_{\mathrm{Cya}}, \theta^1_{\mathrm{Cya}})\,s^+(u_{\mathrm{s}}, \theta_{\mathrm{s}}) \\
&\quad + \kappa^3_{\mathrm{CRP}}\,s^-(x_{\mathrm{Fis}}, \theta^1_{\mathrm{Fis}}) - \gamma_{\mathrm{CRP}}\,x_{\mathrm{CRP}} \\
\dot{x}_{\mathrm{Fis}} &= \kappa^1_{\mathrm{Fis}}\,s^-(x_{\mathrm{Fis}}, \theta^5_{\mathrm{Fis}})\,(1 - s^+(x_{\mathrm{CRP}}, \theta^1_{\mathrm{CRP}})\,s^+(x_{\mathrm{Cya}}, \theta^1_{\mathrm{Cya}})\,s^+(u_{\mathrm{s}}, \theta_{\mathrm{s}})) \\
&\quad + \kappa^2_{\mathrm{Fis}}\,s^+(x_{\mathrm{GyrAB}}, \theta^1_{\mathrm{GyrAB}})\,s^-(x_{\mathrm{TopA}}, \theta^2_{\mathrm{TopA}})\,s^-(x_{\mathrm{Fis}}, \theta^5_{\mathrm{Fis}}) \\
&\quad \times (1 - s^+(x_{\mathrm{CRP}}, \theta^1_{\mathrm{CRP}})\,s^+(x_{\mathrm{Cya}}, \theta^1_{\mathrm{Cya}})\,s^+(u_{\mathrm{s}}, \theta_{\mathrm{s}})) - \gamma_{\mathrm{Fis}}\,x_{\mathrm{Fis}} \\
\dot{x}_{\mathrm{GyrAB}} &= \kappa_{\mathrm{GyrAB}}\,(1 - s^+(x_{\mathrm{GyrAB}}, \theta^2_{\mathrm{GyrAB}})\,s^-(x_{\mathrm{TopA}}, \theta^1_{\mathrm{TopA}}))\,s^-(x_{\mathrm{Fis}}, \theta^4_{\mathrm{Fis}}) - \gamma_{\mathrm{GyrAB}}\,x_{\mathrm{GyrAB}} \\
\dot{x}_{\mathrm{TopA}} &= \kappa_{\mathrm{TopA}}\,s^+(x_{\mathrm{GyrAB}}, \theta^2_{\mathrm{GyrAB}})\,s^-(x_{\mathrm{TopA}}, \theta^1_{\mathrm{TopA}})\,s^+(x_{\mathrm{Fis}}, \theta^4_{\mathrm{Fis}}) - \gamma_{\mathrm{TopA}}\,x_{\mathrm{TopA}} \\
\dot{x}_{\mathrm{rrn}} &= \kappa^1_{\mathrm{rrn}}\,s^+(x_{\mathrm{Fis}}, \theta^3_{\mathrm{Fis}}) + \kappa^2_{\mathrm{rrn}} - \gamma_{\mathrm{rrn}}\,x_{\mathrm{rrn}}
\end{aligned}
$$

According to [2], the following inequality constraints on the parameter values have to be satisfied:

$$0 < \theta^1_{\mathrm{Cya}} < \theta^2_{\mathrm{Cya}},\ \theta^1_{\mathrm{Cya}} < \kappa^1_{\mathrm{Cya}}/\gamma_{\mathrm{Cya}} < \theta^2_{\mathrm{Cya}},\ (\kappa^1_{\mathrm{Cya}} + \kappa^2_{\mathrm{Cya}})/\gamma_{\mathrm{Cya}} > \theta^2_{\mathrm{Cya}}$$
$$0 < \theta^1_{\mathrm{CRP}} < \theta^2_{\mathrm{CRP}},\ \theta^1_{\mathrm{CRP}} < \kappa^1_{\mathrm{CRP}}/\gamma_{\mathrm{Cya}} < \theta^2_{\mathrm{CRP}}$$
$$\theta^1_{\mathrm{CRP}} < (\kappa^1_{\mathrm{CRP}} + \kappa^2_{\mathrm{CRP}})/\gamma_{\mathrm{CRP}} < \theta^2_{\mathrm{CRP}},\ (\kappa^1_{\mathrm{CRP}} + \kappa^3_{\mathrm{CRP}})/\gamma_{\mathrm{CRP}} > \theta^2_{\mathrm{CRP}}$$
$$0 < \theta^1_{\mathrm{Fis}} < \theta^2_{\mathrm{Fis}} < \theta^3_{\mathrm{Fis}} < \theta^4_{\mathrm{Fis}} < \theta^5_{\mathrm{Fis}}$$
$$\theta^1_{\mathrm{Fis}} < \kappa^1_{\mathrm{Fis}}/\gamma_{\mathrm{Fis}} < \theta^2_{\mathrm{Fis}},\ (\kappa^1_{\mathrm{Fis}} + \kappa^2_{\mathrm{Fis}})/\gamma_{\mathrm{Fis}} > \theta^5_{\mathrm{Fis}}$$
$$0 < \theta^1_{\mathrm{GyrAB}} < \theta^2_{\mathrm{GyrAB}},\ \kappa_{\mathrm{GyrAB}}/\gamma_{\mathrm{GyrAB}} > \theta^2_{\mathrm{GyrAB}}$$
$$0 < \theta^1_{\mathrm{TopA}} < \theta^2_{\mathrm{TopA}},\ \kappa_{\mathrm{TopA}}/\gamma_{\mathrm{TopA}} > \theta^2_{\mathrm{TopA}}$$
$$\theta_{\mathrm{rrn}} > 0,\ 0 < \kappa^2_{\mathrm{rrn}}/\gamma_{\mathrm{rrn}} < \theta_{\mathrm{rrn}},\ (\kappa^1_{\mathrm{rrn}} + \kappa^2_{\mathrm{rrn}})/\gamma_{\mathrm{rrn}} > \theta_{\mathrm{rrn}}$$

Moreover, the entry into exponential phase can be simulated by imposing the following initial conditions:

$$x^0_{\mathrm{Cya}} = \theta^2_{\mathrm{Cya}}$$
$$x^0_{\mathrm{CRP}} > \theta^2_{\mathrm{CRP}}$$
$$0 \leq x^0_{\mathrm{Fis}} < \theta^1_{\mathrm{Fis}}$$
$$0 \leq x^0_{\mathrm{GyrAB}} < \theta^1_{\mathrm{GyrAB}}$$
$$0 \leq x^0_{\mathrm{TopA}} < \theta^1_{\mathrm{TopA}}$$
$$0 \leq x^0_{\mathrm{rrn}} < \theta_{\mathrm{rrn}}$$

The following table collects the values for the rate parameters and initial conditions that have been used. These have been chosen from intervals of physiologically realistic values.

Synthesis parameters [M min^{-1}]		Degradation parameters [min^{-1}]		Threshold values [M]		Initial conditions [M]	
κ^1_{Cya}	$3.034 \cdot 10^{-12}$	γ_{Cya}	$4.211 \cdot 10^{-2}$	θ^1_{Cya}	$2.748 \cdot 10^{-11}$	x^0_{Cya}	$2.413 \cdot 10^{-10}$
κ^2_{Cya}	$2.317 \cdot 10^{-11}$	γ_{CRP}	$4.327 \cdot 10^{-3}$	θ^2_{Cya}	$2.413 \cdot 10^{-10}$	x^0_{CRP}	$7.101 \cdot 10^{-6}$
κ^1_{CRP}	$1.553 \cdot 10^{-9}$	γ_{Fis}	$4.261 \cdot 10^{-3}$	θ^1_{CRP}	$1.719 \cdot 10^{-7}$	x^0_{Fis}	$5.000 \cdot 10^{-9}$
κ^2_{CRP}	$1.224 \cdot 10^{-9}$	γ_{GyrAB}	$5.188 \cdot 10^{-3}$	θ^2_{CRP}	$7.753 \cdot 10^{-7}$	x^0_{GyrAB}	$1.614 \cdot 10^{-8}$
κ^3_{CRP}	$1.322 \cdot 10^{-8}$	γ_{TopA}	$6.625 \cdot 10^{-3}$	θ^1_{Fis}	$3.991 \cdot 10^{-8}$	x^0_{TopA}	$2.661 \cdot 10^{-9}$
κ^1_{Fis}	$3.404 \cdot 10^{-10}$	γ_{rrn}	$8.468 \cdot 10^{-3}$	θ^2_{Fis}	$1.888 \cdot 10^{-7}$	x^0_{rrn}	$2.999 \cdot 10^{-6}$
κ^2_{Fis}	$8.668 \cdot 10^{-9}$			θ^3_{Fis}	$3.663 \cdot 10^{-7}$		
κ_{GyrAB}	$9.938 \cdot 10^{-10}$			θ^4_{Fis}	$7.472 \cdot 10^{-7}$		
κ_{TopA}	$2.548 \cdot 10^{-9}$			θ^5_{Fis}	$2.020 \cdot 10^{-6}$		
κ^1_{rrn}	$1.488 \cdot 10^{-7}$			$\theta^1_{\mathrm{GyrAB}}$	$3.991 \cdot 10^{-8}$		
κ^2_{rrn}	$1.506 \cdot 10^{-8}$			$\theta^2_{\mathrm{GyrAB}}$	$1.888 \cdot 10^{-7}$		
				θ^1_{TopA}	$1.221 \cdot 10^{-7}$		
				θ^2_{TopA}	$2.491 \cdot 10^{-7}$		
				θ_{rrn}	$8.898 \cdot 10^{-6}$		
				θ_{s}	0.5		

2 Results of PL identification process

Figure 6 in the main text shows an example of solutions of the PL model obtained by simulation with $T = 10$ min and $SNR = 0.01$. The set of identifiable thresholds associated with all simulations considered in our study is given by

$$\Theta_{\mathrm{id}} = \{\theta^1_{\mathrm{Fis}}, \theta^3_{\mathrm{Fis}}, \theta^4_{\mathrm{Fis}}, \theta^1_{\mathrm{GyrAB}}\} \ .$$

The output of the switch detection and classification algorithms applied to the simulated data in Fig. 6 in the main text is shown in Fig. 1 and Fig. 2, respectively.

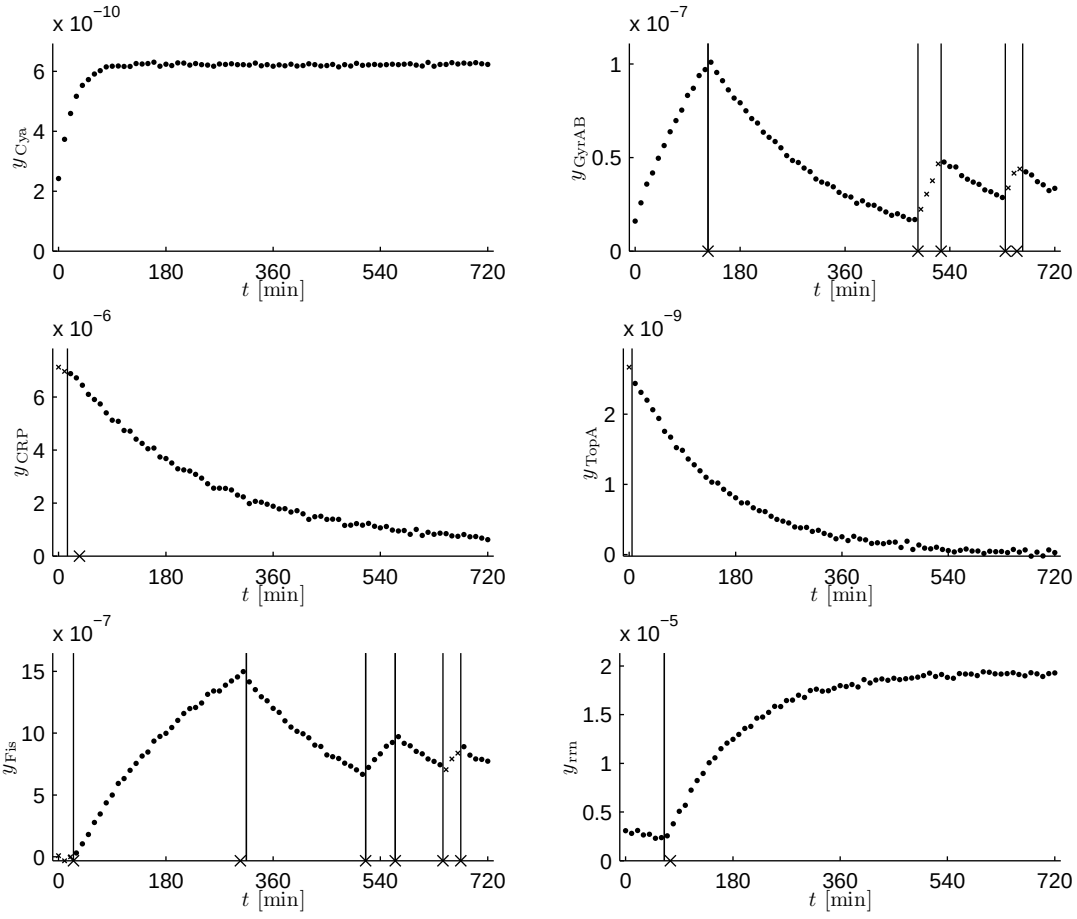

Figure 1: Switch detection results on simulated data for the *E. coli* carbon starvation network. Vertical lines: detected switching times ($\alpha = 0.01$, $l_{\min} = 4$) defining the segments. Crosses on the time axis: real switching times. Data-points represented by small crosses were not attributed to any segment.

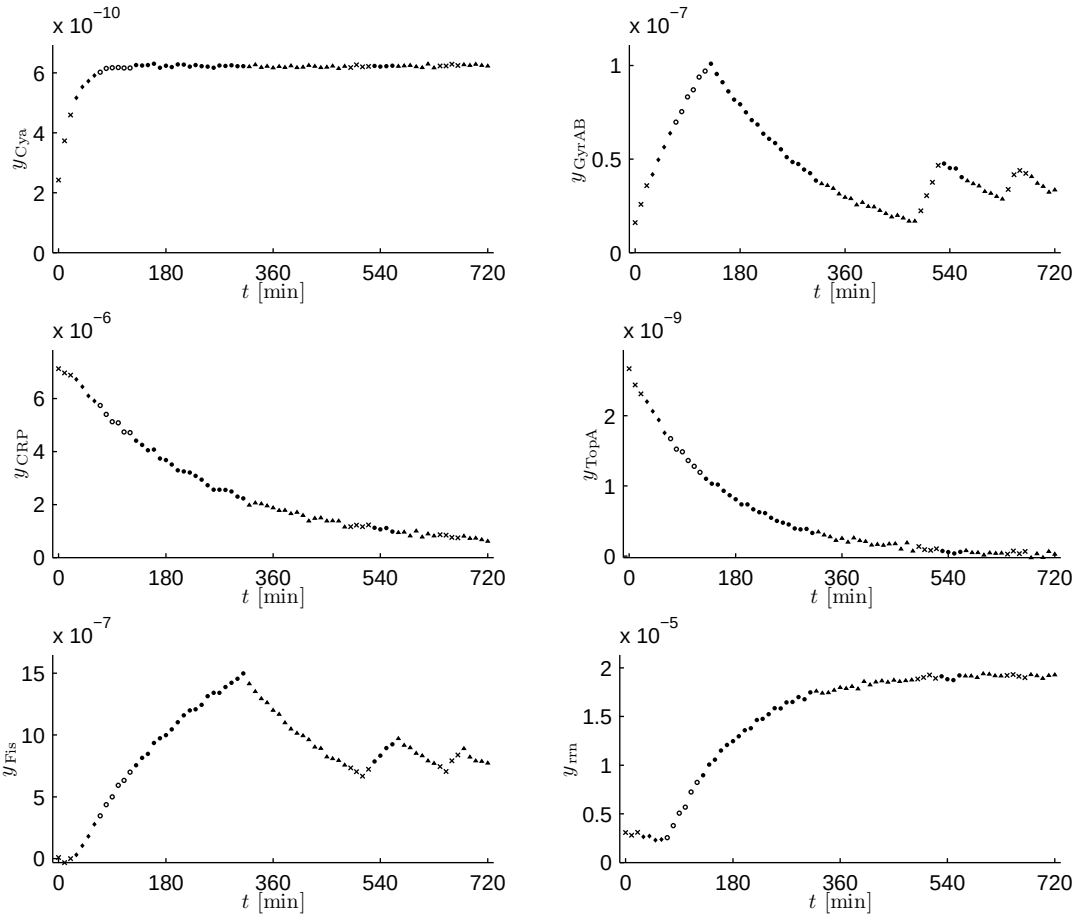

Figure 2: Classification results for $\bar{\alpha} = 0.01$. Same marker denotes data belonging to the same class.

The (maximal) cuts [1] reconstructed for the example in Fig. 1 are reported in the following table, along with their equivalence class and their correctness, as defined in Sec. 4.2 in the main text.

Cut	Regulator	Value [M]	I_{eq} [M]	Correct
$\hat{\theta}^1_{\text{Cya}}$	Cya	$5.899 \cdot 10^{-10}$	$[5.634 \cdot 10^{-10}, 6.165 \cdot 10^{-10}]$	N
$\hat{\theta}^1_{\text{CRP}}$	CRP	$4.498 \cdot 10^{-6}$	$[4.065 \cdot 10^{-6}, 4.932 \cdot 10^{-6}]$	N
$\hat{\theta}^2_{\text{CRP}}$	CRP	$5.746 \cdot 10^{-6}$	$[5.211 \cdot 10^{-6}, 6.281 \cdot 10^{-6}]$	N
$\hat{\theta}^1_{\text{Fis}}$	Fis	$3.118 \cdot 10^{-7}$	$[1.425 \cdot 10^{-7}, 4.810 \cdot 10^{-7}]$	Y
$\hat{\theta}^2_{\text{Fis}}$	Fis	$7.107 \cdot 10^{-7}$	$[5.892 \cdot 10^{-7}, 8.323 \cdot 10^{-7}]$	Y
$\hat{\theta}^1_{\text{GyrAB}}$	GyrAB	$3.975 \cdot 10^{-8}$	$[3.450 \cdot 10^{-8}, 4.501 \cdot 10^{-8}]$	Y
$\hat{\theta}^2_{\text{GyrAB}}$	GyrAB	$6.585 \cdot 10^{-8}$	$[5.378 \cdot 10^{-8}, 7.792 \cdot 10^{-8}]$	N
$\hat{\theta}^1_{\text{TopA}}$	TopA	$1.154 \cdot 10^{-9}$	$[9.513 \cdot 10^{-10}, 1.358 \cdot 10^{-9}]$	N
$\hat{\theta}^2_{\text{TopA}}$	TopA	$1.723 \cdot 10^{-9}$	$[1.444 \cdot 10^{-9}, 2.002 \cdot 10^{-9}]$	N
$\hat{\theta}^1_{\text{rrn}}$	stable RNAs	$3.396 \cdot 10^{-6}$	$[2.507 \cdot 10^{-6}, 4.286 \cdot 10^{-6}]$	N
$\hat{\theta}^2_{\text{rrn}}$	stable RNAs	$8.659 \cdot 10^{-6}$	$[6.752 \cdot 10^{-6}, 1.057 \cdot 10^{-5}]$	N

The following table shows all minimal multicuts produced by the identification procedure, along with the correctness of the cuts composing each multicut, from which one can easily compute the F-measures. In particular, the best multicut is M_{13}, characterized by an F-measure of $6/7 \simeq 0.86$.

Multicut	Cuts	Correct
M_1	$\{\hat{\theta}^1_{\text{Cya}}, \hat{\theta}^1_{\text{CRP}}, \hat{\theta}^1_{\text{GyrAB}}\}$	{N,N,Y}
M_2	$\{\hat{\theta}^1_{\text{Cya}}, \hat{\theta}^2_{\text{Fis}}, \hat{\theta}^1_{\text{GyrAB}}\}$	{N,Y,Y}
M_3	$\{\hat{\theta}^1_{\text{Cya}}, \hat{\theta}^1_{\text{GyrAB}}, \hat{\theta}^1_{\text{TopA}}\}$	{N,Y,N}
M_4	$\{\hat{\theta}^1_{\text{Cya}}, \hat{\theta}^1_{\text{GyrAB}}, \hat{\theta}^2_{\text{rrn}}\}$	{N,Y,N}
M_5	$\{\hat{\theta}^1_{\text{CRP}}, \hat{\theta}^2_{\text{CRP}}, \hat{\theta}^1_{\text{GyrAB}}\}$	{N,N,Y}
M_6	$\{\hat{\theta}^1_{\text{CRP}}, \hat{\theta}^1_{\text{Fis}}, \hat{\theta}^1_{\text{GyrAB}}\}$	{N,Y,Y}
M_7	$\{\hat{\theta}^1_{\text{CRP}}, \hat{\theta}^1_{\text{GyrAB}}, \hat{\theta}^2_{\text{GyrAB}}\}$	{N,Y,N}
M_8	$\{\hat{\theta}^1_{\text{CRP}}, \hat{\theta}^1_{\text{GyrAB}}, \hat{\theta}^2_{\text{TopA}}\}$	{N,Y,N}
M_9	$\{\hat{\theta}^1_{\text{CRP}}, \hat{\theta}^1_{\text{GyrAB}}, \hat{\theta}^1_{\text{rrn}}\}$	{N,Y,N}
M_{10}	$\{\hat{\theta}^2_{\text{CRP}}, \hat{\theta}^2_{\text{Fis}}, \hat{\theta}^1_{\text{GyrAB}}\}$	{N,Y,Y}
M_{11}	$\{\hat{\theta}^2_{\text{CRP}}, \hat{\theta}^1_{\text{GyrAB}}, \hat{\theta}^1_{\text{TopA}}\}$	{N,Y,N}
M_{12}	$\{\hat{\theta}^2_{\text{CRP}}, \hat{\theta}^1_{\text{GyrAB}}, \hat{\theta}^2_{\text{rrn}}\}$	{N,Y,N}
M_{13}	$\{\hat{\theta}^1_{\text{Fis}}, \hat{\theta}^2_{\text{Fis}}, \hat{\theta}^1_{\text{GyrAB}}\}$	{Y,Y,Y}
M_{14}	$\{\hat{\theta}^1_{\text{Fis}}, \hat{\theta}^1_{\text{GyrAB}}, \hat{\theta}^1_{\text{TopA}}\}$	{Y,Y,N}
M_{15}	$\{\hat{\theta}^1_{\text{Fis}}, \hat{\theta}^1_{\text{GyrAB}}, \hat{\theta}^2_{\text{rrn}}\}$	{Y,Y,N}
M_{16}	$\{\hat{\theta}^2_{\text{Fis}}, \hat{\theta}^1_{\text{GyrAB}}, \hat{\theta}^2_{\text{GyrAB}}\}$	{Y,Y,N}
M_{17}	$\{\hat{\theta}^2_{\text{Fis}}, \hat{\theta}^1_{\text{GyrAB}}, \hat{\theta}^2_{\text{TopA}}\}$	{Y,Y,N}
M_{18}	$\{\hat{\theta}^2_{\text{Fis}}, \hat{\theta}^1_{\text{GyrAB}}, \hat{\theta}^1_{\text{rrn}}\}$	{Y,Y,N}
M_{19}	$\{\hat{\theta}^1_{\text{GyrAB}}, \hat{\theta}^2_{\text{GyrAB}}, \hat{\theta}^1_{\text{TopA}}\}$	{Y,N,N}
M_{20}	$\{\hat{\theta}^1_{\text{GyrAB}}, \hat{\theta}^2_{\text{GyrAB}}, \hat{\theta}^2_{\text{rrn}}\}$	{Y,N,N}
M_{21}	$\{\hat{\theta}^1_{\text{GyrAB}}, \hat{\theta}^1_{\text{TopA}}, \hat{\theta}^2_{\text{TopA}}\}$	{Y,N,N}
M_{22}	$\{\hat{\theta}^1_{\text{GyrAB}}, \hat{\theta}^1_{\text{TopA}}, \hat{\theta}^1_{\text{rrn}}\}$	{Y,N,N}
M_{23}	$\{\hat{\theta}^1_{\text{GyrAB}}, \hat{\theta}^2_{\text{TopA}}, \hat{\theta}^2_{\text{rrn}}\}$	{Y,N,N}
M_{24}	$\{\hat{\theta}^1_{\text{GyrAB}}, \hat{\theta}^1_{\text{rrn}}, \hat{\theta}^2_{\text{rrn}}\}$	{Y,N,N}

References

[1] S. Drulhe, G. Ferrari-Trecate, and H. de Jong. Reconstruction of switching thresholds in piecewise-affine models of genetic regulatory networks. *IEEE Trans. Automat. Control*, 53(1):153–165, 2008.

[2] D. Ropers, H. de Jong, M. Page, D. Schneider, and J. Geiselmann. Qualitative simulation of the carbon starvation response in *Escherichia coli*. *Biosystems*, 84(2):124–152, 2006.